1 **JAST (Journal of Animal Science and Technology) TITLE PAGE**

2 **Upload this completed form to website with submission**

3

ARTICLE INFORMATION	Fill in information in each box below
Article Type	Research article
Article Title (within 20 words without abbreviations)	Mechanism of holocarboxylase synthetase and biotin supplementation in promoting adipose development
Running Title (within 10 words)	Holocarboxylase synthetase and biotin supplementation in promoting adipose development
Author	Lei Qin(first author) 1, Yuxing Dai (first author)1, Chunguang Zhang 1, Yunyan Luo 1, Shifan Deng 1, Han Chu 1, Liang Hong 1, Jianbin Zhang 1, Hua Yang 1, Gaoxiao Xu (corresponding author) 3, *, Fuping Zhao(corresponding author) 4, Lei Pu (corresponding author)1,2
Affiliation	1 Tianjin Key Laboratory of Agricultural Animal Breeding and Healthy Husbandry, College of Animal Science and Veterinary Medicine, Tianjin Agricultural University, Tianjin 300384, China 2 Tianjin modern Tianjiao Agricultural Technology Co., LTD，Tianjin Key Laboratory of Green Ecological Feed, Tianjin, China 3 Anhui Province Key Laboratory of Embryo Development and Reproductive Regulation, Anhui Province Key Laboratory of Environmental Hormone and Reproduction, School of Biological and Food Engineering, Fuyang Normal University, Fuyang, 236037, China 4 Institute of Animal Science, Chinese Academy of Agricultural Sciences, Beijing 100193, China
ORCID (for more information, please visit https://orcid.org)	Lei Qin (https://orcid.org/0000-0002-3934-421X) Yuxing Dai (https://orcid.org/0009-0002-1805-3824) Chunguang Zhang (https://orcid.org/0009-0009-2367-1652) Yunyan Luo (https://orcid.org/0009-0002-3267-7924) Shifan Deng (https://orcid.org/0009-0002-8158-8784) Han Chu (https://orcid.org/0009-0002-6364-5618) Liang Hong (https://orcid.org/0000-0003-3876-8819) Jianbin Zhang (https://orcid.org/0000-0001-5773-0045) Hua Yang (https://orcid.org/0000-0003-2007-9994) Gaoxiao Xu (https://orcid.org/0009-0000-1101-8490) Fuping Zhao (https://orcid.org/0009-0001-8735-1000) Lei Pu (https://orcid.org/0000-0002-0825-7658)
Competing interests	No potential conflict of interest relevant to this article was reported.
Funding sources State funding sources (grants, funding sources, equipment, and supplies). Include name and number of grant if available.	This work was supported by Key R&D Project in Hainan Province (ZDYF2024XDNY271), Tianjin Science and Technology Plan Project (23ZYCGSN00230), National Swine Industry Technology System (CARS-35), Anhui Natural Science Foundation Project (2208085MC76), the Scientific Research Program of Tianjin Education Commission, China (2018KJ188), Fuyang Normal University scientific research platform open topic (FYKFKT24042).
Acknowledgements	Not applicable.
Availability of data and material	Upon reasonable request, the datasets of this study can be available from the corresponding author.
Authors' contributions Please specify the authors' role using this form.	Conceptualization: Pu L Data curation: qin L, dai XY Formal analysis: qin L, Hong L, Zhang BJ, Yang H, Pu L Methodology: qin L, dai XY, Zhang GC, Luo YY, Deng FS, Chu H Validation: qin L, Xu XG Investigation: Zhao PF, Pu L Writing - original draft: qin L, dai XY Writing - review & editing: qin L, dai XY, Zhang GC, Luo YY, Deng FS, Chu H, Hong L, Zhang BJ, Yang H, Xu XG, Zhao PF, Pu L

Ethics approval and consent to participate	This manuscript has been approved by the IACUC.

CORRESPONDING AUTHOR CONTACT INFORMATION

For the corresponding author (responsible for correspondence, proofreading, and reprints)	**Fill in information in each box below**
First name, middle initial, last name	Lei Pu
Email address – this is where your proofs will be sent	pulei87@126.com
Secondary Email address	qinlei98517@163.com
Address	Tianjin Agricultural University
Cell phone number	13716169331
Office phone number	23792065
Fax number	23792065

Abstract

Pig back fat (BF) thickness is a key indicator for evaluating lipid deposition in pigs. Consuming pork belly with thick BF can increase cholesterol intake and negatively impact human health. Holocarboxylase synthetase (HLCS) is a crucial ligase that binds biotin to carboxylases, affecting the function of biotin-dependent carboxylases. The relationship between single-nucleotide polymorphisms (SNPs) in *HLCS* and BF in pigs, along with the direct effects of *HLCS* on adipocyte development, remains unclear. While biotin is used to treat HLCS deficiency, its role in adipocyte development is not well understood. This study identified two *HLCS* SNPs associated with 100-kg BF in 592 Duroc pigs. In 3T3-L1 cells, *HLCS* interference reduced cell proliferation and decreased protein levels of phosphorylated p38 (p-p38) and phosphorylated signal-regulated kinase1/2 (p-ERK1/2) in the MAPK signaling pathway. Exogenous biotin promoted *HLCS* expression and alleviated the inhibitory effects of *HLCS* interference on lipogenesis-related genes, lipolysis-related genes, glycolysis-related genes, and p-ERK1/2 and p-p38 protein expression in adipocytes. In conclusion, *HLCS* is a significant candidate gene for pig BF development, with its interference adversely affecting adipocyte growth. Exogenous biotin not only stimulated HLCS expression but also influenced lipid metabolism by regulating carboxylase activity, glycolysis, and lipid synthesis/degradation through the MAPK pathway. This study provides new insights into HLCS function and the therapeutic role of biotin in HLCS deficiency, offering a theoretical foundation for molecular breeding of pigs with reduced BF.

Keywords

HLCS gene; biotin; single-nucleotide polymorphism; adipose development; MAPK signaling pathway

Introduction

Pork is an important source of meat for humans [1]. Back fat (BF) is the fat that covers the back of domestic animals. Compared with other domestic animals, BF in pigs is thicker [2]. Pig BF contains significant amounts of lipids, mainly triglycerides and cholesterol, and is therefore considered a high-calorie food [3]. Consuming too much cholesterol can adversely affect human health, leading to diseases such as obesity, atherosclerotic cardiovascular disease, and myocardial infarction [4]. Therefore, breeding pigs with low BF has great significance for improving meat quality and human health.

Holocarboxylase synthetase (HLCS) is an enzyme that catalyzes the covalent binding of biotin to carboxylase, leading to carboxylase biotinylation [5, 6]. Biotin-dependent carboxylases mainly include pyruvate carboxylase (PC), 3-methylcrotonyl-CoA carboxylase (MCC), propionyl-CoA carboxylase (PCC), and acetyl-CoA carboxylase (ACC) [7]. These biotin-dependent carboxylases play a critical role in fatty acid synthesis, amino acid metabolism, and degradation of odd-chain fatty acids, respectively [8-11]. It has been found that knockdown of *HLCS* in the breast cancer cell line MCF-7 and the highly invasive cell line MDA-MB-231 results in decreased biotinylation of ACC and PC [12]. Therefore, HLCS has the potential to regulate fatty acid metabolism. Genome-wide association study data revealed that SNPs significantly associated with residual feed intake, defined as the difference between observed and predicted feed intake based on average daily gain and BF, are located within the *HLCS* gene [13]. However, the relationship between SNPs of the *HLCS* gene and BF in pigs has not been studied, and the direct effects of *HLCS* on adipocyte development have not been reported in detail.

HLCS can catalyze the covalent binding of biotin to carboxylases [7]. Clinical studies have shown that mutations in the *HLCS* gene can lead to HLCS deficiency, which is associated with various uncomfortable symptoms. Studies have shown that symptoms of HSCS deficiency can improve with oral biotin supplementation [14, 15]. Biotin is a water-soluble vitamin and an essential micronutrient for animal growth. In one study, researchers found that the total fat content in the sole horn was significantly higher in biotin-supplemented cows than in control cows [16]. When rats on a high-fat diet were supplemented with biotin, peroxisome proliferator-activated receptor gamma (PPARγ), a key regulator of adipogenesis, was promoted [17]. Thus, biotin is considered an adipogenic agent with the ability to coordinate lipid and amino acid metabolism in adipocytes [18]. Biotin is also used as a treatment for HLCS deficiency. However, the molecular mechanism by which biotin treats HLCS deficiency remains unclear.

Therefore, the purpose of this study was to investigate the correlation between SNPs of *HLCS* and BF at 100 kg in pigs and to explore the direct effect of *HLCS* interference on adipocytes, as well as to study the molecular mechanism of biotin compensation under HLCS deficiency.

Materials and methods

Animals and data collection

A total of 592 Duroc pigs were allowed to feed ad libitum using the Osborne automated feeding system (OSBORN-FIRE, US), and prior to this, they underwent an adaptation period of approximately 7 days. The basal diet was formulated to meet or exceed National Research Council standards. The specific feed formulation and

nutritional composition can be found in Supplementary Table S1. Parity, batch, and paternity information of the Duroc pigs were recorded. The experiment lasted from 90 days of age to 180 days of age. The initial weight of the Duroc pigs at 90 days of age was recorded. When the pigs reached approximately 100 kg, BF thickness was measured between the 10th and 11th ribs using an Aloca ultrasonic meter (Corometrics Medical Systems, Inc., Wallingford, CT, USA), and body weight was measured at the same time. BF measurements at 100 kg were adjusted to the target body weight of 100 kg.

Collected pig ear samples. Genomic DNA for the genotypic was extracted from ear samples by the phenol-chloroform procedure. DNA samples were stored at -20℃. The 592 Duroc pigs were genotyped using the Illumina Porcine SNP60 Bead Chip (Illumina, San Diego, CA, USA). Infinium II multicopy technology was applied in this experiment. SNP chips were scanned using iScan, and data were analyzed with Illumina Genome Studio (Illumina).

The RNA-seq results of adipose tissue from 592 Duroc pigs with CC and TT genotypes of the *HLCS* (ASGA0089950) gene were analyzed.

3T3-L1 cell culture and adipogenic differentiation

The 3T3-L1 cells (the Swine Genetics and Breeding Innovation Team at the Institute of Animal Science, Chinese Academy of Agricultural Sciences, Beijing.) were removed from liquid nitrogen storage and immediately transferred to a 38°C water bath for recovery. Dulbecco's modified Eagle medium, supplemented with 10% fetal bovine serum (Gibco, Grand Island, NY, USA) and 100 units/mL penicillin-streptomycin (Solarbio, Beijing, China), was used for cell culture in an incubator with 5% CO_2 at 37°C. When the 3T3-L1 cells reached 80% confluence, the medium was aspirated, and the cells were rinsed with phosphate-buffered saline (PBS) (Solarbio, Beijing, China). For digestion, 2 mL of 0.25% trypsin (Solarbio, Beijing, China) was added and then incubated for 3–5 min, and an equal amount of medium was added to stop the digestion. The cell suspension was then transferred to a centrifuge tube, then centrifuged for 5 min. The supernatant was removed, and fresh medium was added and mixed by pipetting. The cell culture medium was refreshed daily, and the cells were passaged at a 1:3 ratio. Adipogenic induction began the day after contact inhibition. For adipogenic differentiation, the medium contained 0.5 mg/L dexamethasone (Sigma, Germany), 0.5 mmol/L IBMX (Sigma, Germany), and 10 μg/mL insulin (Sigma, Germany) for the first 2 days, followed by culture in a medium supplemented with 10 μg/mL insulin. The cells were cultured in this medium for 4 days, followed by subsequent treatment.

Transfection of cell with siRNA

HLCS small interfering RNA (siRNA) and negative control (NC) siRNA oligonucleotides are provided in Supplementary Table S2. Cells were transfected using Lipofectamine 3000 transfection reagent according to the manufacturer's protocol. Two hours before transfection, the cell medium was replaced with Opti-MEM medium (Gibco, Grand Island, NY, USA). The siRNA (20 μM) was incubated with 5 μL of Lipofectamine 3000 in Opti-MEM medium for 20 min at room temperature prior to transfection. Six hours later, the medium was replaced with complete medium.

EdU detection

After passaging, the cells were cultured for 24 h for EdU proliferation detection. For this assay, 10 μM EdU was added to the growth medium and incubated for 2 h. Fixation, permeabilization, and EdU staining were

performed according to the manufacturer's protocol (Beyotime, Shanghai, China). Cell nuclei were counterstained with Hoechst 33342 at a concentration of 5 μg/mL for 10 min. EdU-positive cells were then observed under a fluorescence microscope (Motic, Xiamen, China) to estimate the ratio of EdU-positive cells (EdU-stained cells/total cells).

Oil Red O staining

Cells were cultured to the terminal differentiation stage, and adipocytes were washed three times with PBS. A 4% cell fixation solution (Sigma, Germany) was then added, and the cells were fixed in a 37°C incubator for 45 min. After washing three times with PBS, Oil Red O (Sigma, Germany) solution was added for 45 min. The staining of lipid droplets was observed under a microscope, and after taking images, Oil Red O was washed out with isopropanol. Absorbance was measured using a microplate reader at a wavelength of 510 nm.

Bodipy staining

Cells were cultured to the terminal differentiation stage, and adipocytes were washed three times with PBS. A 4% cell fixation solution was added, and the cells were fixed in a 37°C incubator for 45 min. After washing three times with PBS, Bodipy (Thermo, Shanghai, China) staining was performed for 45 min. The staining of lipid droplets was recorded under a microscope, and the amount of Bodipy fluorescence was quantified using ImageJ software.

RNA extraction and quantitative real-time polymerase chain reaction (qRT-PCR)

Total RNA was extracted using the RNA extraction kit (TRIzol reagent; TaKaRa Company), and the extraction steps were performed according to the instructions of the kit. The resulting RNA solution was stored at a temperature of −80°C. The RNA was then immediately reverse-transcribed into cDNA using a reverse transcription kit (TaKaRa), following the kit instructions. The synthesized cDNA was stored at −20°C or directly at −80°C for later use.

Primers were designed using primer software, and the primer sequences are shown in Supplementary Table S3. qRT-PCR was performed to detect gene expression. In an eight-row qRT-PCR tube, the following components were added in sequence: 2× All-in-One qPCR Mix 7.5 μL, cDNA 1 μL, upstream primer 0.75 μL, downstream primer 0.75 μL, and ddH_2O 5 μL. These components were used to prepare the qPCR reaction solution, which was then centrifuged and mixed.

The PCR reaction was conducted as follows: pre-denaturation at 95°C for 10 min, denaturation at 95°C for 30 s, annealing at 58°C for 30 s, and extension at 72°C for 30 s. This cycle was repeated 45 times, followed by melting curve analysis (for melting curve analysis: 95°C for 2 min, 72°C for 1 min, and 95°C for 30 s).

Western blotting analysis

Cells were harvested and lysed in RIPA buffer supplemented with a protease inhibitor (Roche Complete Mini tablet) and phosphatase inhibitor (Pierce Halt phosphatase inhibitor cocktail) to prepare whole-cell extracts. The lysates were centrifuged at 12,000 rpm for 10 min, and the supernatant was boiled in sodium dodecyl sulfate loading buffer (Beyotime, Shanghai, China). Proteins were separated using 12.5% sodium dodecyl sulfate–polyacrylamide gel electrophoresis and transferred to a polyvinylidene difluoride transfer membrane (Solarbio, Beijing, China). The membrane was blocked with 5% defatted milk and incubated overnight at 4°C with primary

antibodies, followed by horseradish peroxidase-conjugated secondary antibody. Blots were visualized using a commercial enhanced chemiluminescence detection kit (Solarbio, Beijing, China), with glyceraldehyde-3-phosphate dehydrogenase (GAPDH) as an internal control for normalization.

Data analysis

Allele and genotype frequencies were obtained for each polymorphism. Statistical analyses were performed for genotypic frequencies, heterozygosity (*He*), effective allele numbers (*Ne*), polymorphism information content (*PIC*), and Hardy–Weinberg equilibrium. The genetic haplotype definition was defined as a group of genes or SNPs that are statistically associated with each other, forming a gene locus or common pattern of genetic variation. Haploview 4.2 (http://www.broadinstitute.org/mpg/haploview) (accessed on 8 September 2021) was used to detect haplotype blocks in all the SNPs of the *HLCS* gene [19].

The generalized linear model program in SAS 9.2 was used to conduct least squares variance analysis with the following model to compare the significance of SNPs and growth performance:

$$Y = \mu + G + S + W + e,$$

where Y is the observation of the traits, μ is the population mean, G is the genotype effect, S is the sex fixation effect, W is the initial weight, and e is the random error.

The MTDFREML program was used to obtain the estimated breeding value of the 100-kg BF. Depending on the trait, the mixed model for a single trait is:

$$y_{ijk} = \mu + S_i + P_i + b_i + O_j + S_j + e_{ijk},$$

where y is the observation of the traits, μ is the population mean, S_i is the sex fixation effect, P_i is the parity fixation effect, b_i is the batch fixation effect, O_j is the individual animal random effect, S_j is the second animal effect (father number), and e_{ijk} is the random error.

Three biological replicates were set up in each experiment. For cellular experiments, qRT-PCR and western blotting results were analyzed using the $2^{-\Delta\Delta Ct}$ method. Data analysis was conducted with an independent-samples *t*-test, one-way and two-way analysis of variance using SPSS 25 software. The results of the two-way analysis of variance were presented in the Supplementary Table S4-S5. For significance testing, $P < 0.01$ indicates a highly significant difference, $P < 0.05$ indicates a significant difference, and $P > 0.05$ indicates an insignificant difference. The data in the tables are shown as mean ± standard error, and the data in the figures are expressed as mean ± standard deviation. Proteins were analyzed in grayscale using ImageJ software to obtain quantitative data.

Results

HLCS genotype frequencies and haplotype determination

In total, 592 Duroc pigs were randomly selected for descriptive statistics of 100-kg BF. The 100-kg BF value was 7.89 mm. Analysis of the coefficient of variation provided insight into data dispersion, with a coefficient of variation of 0.20 for 100-kg BF. The whole genome was categorized using the Illumina SNP60 chip, and SNP loci within, before, and after the *HLCS* gene were identified and compared using Ensembl software. The genotype frequencies and genetic diversity of five SNPs of the *HLCS* gene are shown in Table 1. All selected genetic variants were in Hardy–Weinberg equilibrium.

This study found linkage among five SNPs of *HLCS*. Based on these five SNPs, two haplotype blocks were detected in Duroc pigs (Fig. 1). ASGA0089950 and ASGA0097399 showed high linkage, while ALGA0073814 was highly linked with ASGA0059961 and ALGA0073818.

Association of HLCS genotype with 100-kg BF traits and expression analysis of related genes in Duroc pigs

This experiment included a joint analysis of phenotype values and estimated breeding values to examine the correlation between five SNPs of the *HLCS* gene and 100-kg BF in 592 Duroc pigs. The results of the correlation analysis are shown in Table 2. For ASGA0089950, individuals with the CT genotype showed significantly thinner 100-kg BF than those with CC or TT genotypes. For ASGA0097399, individuals with the CG genotype had significantly thinner 100-kg BF than those with CC or GG genotypes. For ALGA0073814, ALGA0073814, and ALGA0073818, different genotypes did not have a significant effect on 100-kg BF.

The mRNA expression of *HLCS* and related carboxylases in the adipose tissue of Duroc pigs was measured (Fig. 2). The results showed that the expression of *HLCS*, *ACC1*, *PCC*, and *MCC* in individuals with the CC genotype was lower than in those with the TT genotype in ASGA0089950. Therefore, this study suggests that mutation of the *HLCS* gene is closely associated with 100-kg BF in pigs.

Interference with HLCS inhibited 3T3-L1 cell proliferation

We investigated *HLCS* expression during 3T3-L1 cell proliferation. *HLCS* gene expression was measured at 0, 12, 24, 36, 48, and 60 h of 3T3-L1 cell proliferation. As the 3T3-L1 cells proliferated, *HLCS* expression increased rapidly, peaking at 12 h and then beginning to decline, showing an initial increase followed by a decrease (Fig. 3A). The 3T3-L1 cells were transfected with two different siRNAs targeting *HLCS*. Compared with the control group, no significant change in *HLCS* mRNA expression was observed in the *siRNA-1* group, while *HLCS* mRNA expression was significantly reduced in the *siRNA-2* group. Thus, *siRNA-2* was selected for *HLCS* interference (Fig. 3B).

After *HLCS* interference, the proliferation of 3T3-L1 cells was assessed by EdU staining. Interference with *HLCS* significantly reduced the proliferation rate of 3T3-L1 cells (Fig. 3C). These results indicate that cell proliferation was inhibited following *HLCS* interference. Additionally, after *HLCS* interference, mRNA expression of *cyclin-dependent kinase inhibitor 1A (P21)* was upregulated, while *cyclin-dependent kinase 2 (CDK2)* and *cyclin-dependent kinases B (Cyclin B)* were downregulated (Fig. 3D). The protein expression of CDK2 followed a similar trend to its mRNA expression (Fig. 3E). In summary, these data suggest that 3T3-L1 cell proliferation decreased upon *HLCS* interference.

To determine whether MAPK pathways were involved in 3T3-L1 cell proliferation after *HLCS* interference, protein levels of phosphorylation c-Jun N-terminal kinase (p-JNK), JNK, p-p38, p38, p-ERK1/2, and ERK1/2 were examined by western blotting. The results showed that *siHLCS* transfection markedly decreased p-p38 and p-ERK1/2 levels (Fig. 3F). However, JNK and p-JNK expression was notably low in proliferating 3T3-L1 cells (Supplementary Fig. S1). These results suggest that the ERK1/2 and p38 signaling pathways are inhibited in 3T3-L1 cell proliferation following *HLCS* interference.

siHLCS inhibited adipogenic differentiation of 3T3-L1 cells

qRT-PCR was used to analyze the expression of the *HLCS* gene at different stages of adipogenic differentiation on days 0, 2, 4, 6, and 8 in 3T3-L1 cells. The results showed that *HLCS* mRNA expression increased rapidly in the early stages of adipogenic differentiation, peaking on day 2 and then gradually declining (Fig. 4A). Compared with the NC group, Oil Red O absorbance showed a downward trend following *siHLCS* transfection (Fig. 4B). Bodipy staining results indicated that compared with the NC group, the number of lipid droplets was significantly reduced after *siHLCS* transfection, as evidenced by a quantitative decrease in Bodipy fluorescence (Fig. 4C). After *HLCS* interference, cells were collected on day 6 following induction of adipogenic differentiation. The results confirmed that *HLCS* mRNA expression was significantly downregulated after *siHLCS* transfection compared with the NC group. mRNA expression of adipogenic-related genes, including *peroxisome proliferator-activated receptors γ (PPARγ)*, *fatty acid binding proteins (AP2), fatty acid synthase (FAS), and CCAAT/enhancer binding protein α (CEBPα),* was also significantly downregulated following *HLCS* interference (Fig. 4D). Western blotting analysis revealed that protein levels of FAS, PPARγ, CEBPα, and AP2 were significantly lower in the *HLCS* interference group than in the NC group (Fig. 4E). In summary, these data suggest that adipogenic differentiation of 3T3-L1 cells was inhibited following *HLCS* interference.

Exogenous biotin promoted expression of HLCS and alleviated inhibition of adipogenic differentiation by interfering with HLCS in 3T3-L1 cells

HLCS catalyzes the covalent attachment of biotin to carboxylases. It was observed that HLCS expression significantly increased following the addition of 1 μM biotin (Fig. 5A). Adipogenic differentiation of adipocytes increased with different concentrations of exogenous biotin, with 1 μM biotin showing the most effective results overall (Supplementary Fig. S2). Therefore, 1 μM biotin was selected for subsequent experiments.

To investigate the effect of biotin on adipogenic differentiation in 3T3-L1 cells with *HLCS* interference, we applied a combined treatment to establish four treatment groups: NC group, *siHLCS* group, Biotin group, and *siHLCS* + Biotin group. 3T3-L1 cells were induced to undergo adipogenic differentiation for 6 days. Cells were stained with Oil Red O, extracted with isopropanol, and quantified by absorbance measurement at 510 nm. Lipid accumulation was significantly increased in the Biotin group compared with the NC group. In the *siHLCS* + Biotin group, lipid accumulation showed an increasing trend compared with the *siHLCS* group, although the difference was not significant (Fig. 5B, C).

Bodipy staining was also performed on 3T3-L1 cells (Fig. 5D). The fluorescence intensity of lipid droplets was analyzed using ImageJ software (Fig. 5E). Compared with the NC group, fluorescence intensity was significantly increased in the Biotin group and significantly decreased in the *siHLCS* group. The *siHLCS* + Biotin group showed significantly higher fluorescence intensity compared with the *siHLCS* group.

On day 6 of adipogenic differentiation, mRNA was extracted from cells in each treatment group, and qRT-PCR was used to measure *HLCS*, *FAS*, *PPARγ*, *CEBPα*, and *AP2* gene expression. Compared with the NC group, mRNA expression of *HLCS*, *PPARγ*, *CEBPα*, and *AP2* was significantly upregulated in the Biotin group. In the *siHLCS* + Biotin group, mRNA expression of *HLCS*, *PPARγ*, and *CEBPα* was significantly upregulated compared with the *siHLCS* group (Fig. 5F).

Protein expression levels of HLCS, FAS, PPARγ, CEBPα, and AP2 were analyzed by western blotting (Fig. 5G). Compared with the NC group, AP2 protein levels were significantly upregulated in the Biotin group. In the

siHLCS + Biotin group, protein expression of FAS and PPARγ was upregulated compared with the *siHLCS* group, while the levels of other proteins showed no significant differences.

In summary, these results indicate that exogenous biotin can promote adipogenic differentiation and mitigate the inhibitory effect of *HLCS* interference on adipogenic differentiation in 3T3-L1 cells.

Effect of biotin combined with HLCS on carboxylase, lipolysis, glycolysis, and MAPK signaling pathway after adipogenic differentiation of 3T3 cells

HLCS catalyzes the binding of biotin to carboxylases (Fig. 6A). To investigate the molecular mechanisms of biotin and *HLCS* effects on adipogenic differentiation of 3T3-L1 cells, expression levels of several enzymes were measured. The results showed that after biotin addition, ACC1 and ACC2 expression levels increased, while PC, MCC, and PCC expression levels decreased. When *HLCS* was interfered with, the expression of ACC1, PC, MCC, and PCC decreased. In *HLCS*-interfered 3T3-L1 cells, the addition of biotin increased the expression of ACC1, PC, MCC, and PCC (Fig. 6B, C).

This study found that expression of perilipin 2 (PLIN2), lipoprotein lipase (LPL), adipose triglyceride lipase (ATGL), and hormone-sensitive lipase (HSL) decreased after treatment with exogenous biotin or *HLCS* interference compared with the NC group. In *HLCS*-interfered 3T3-L1 cells, adding biotin significantly increased the expression of PLIN2, LPL, ATGL, and HSL compared with cells without biotin (Fig. 6D, E). Compared with the NC group, expression levels of *glycogen synthase kinase-3β* (*GSK3β*), *pyruvate kinase M (PKM)*, and *protein kinase, AMP-activated, γ3* (*PRKAG3)* significantly increased after biotin treatment and significantly decreased following *HLCS* interference. In the *siHLCS* + Biotin group, *GSK3β*, *PKM*, and *PRKAG3* levels increased compared with the *siHLCS* group in 3T3-L1 cells (Fig. 6F, G).

In addition, the protein expression of p-ERK1/2 and p-p38 significantly decreased after biotin treatment, while ERK1/2 protein expression increased. The ratios of p-ERK1/2 to ERK1/2 and p-p38 to p38 also decreased after biotin treatment and *HLCS* interference. However, in the *siHLCS* + Biotin group, the protein expression of p-p38 and p-ERK1/2 was significantly higher than in the *siHLCS* group (Fig. 6H).

Discussion

BF is an important economic trait in pigs and a key target for genetic breeding improvement [20-23]. The 100-kg BF trait represents the fat thickness in pigs at a weight of 100 kg, indicating their fat deposition ability [24, 25]. In this study, five SNPs were identified within the *HLCS* gene, located on chromosome 13 in the intron region. These five SNPs showed high linkage, and two of them were correlated with 100-kg BF in the Duroc pig population. This finding supports the idea that the *HLCS* gene may play a key role in influencing fat deposition.

It is well known that the genome contains millions of SNPs, allowing for intraspecies genome variation [26, 27]. Many SNPs are distributed within intron regions, and some of these intronic SNP mutations lead to abnormal splicing, which can result in lesions [27, 28]. Potentially affecting *HLCS* gene expression. This study also confirmed that *HLCS* SNPs were related to changes in *HLCS* mRNA expression. Rather than focusing solely on how SNPs affect *HLCS* gene expression, this study suggests that it is more meaningful to investigate how changes in *HLCS* gene expression impact adipocyte development. Furthermore, understanding how SNPs affect gene

expression is essential for determining practical applications once the function of the *HLCS* gene is established. Therefore, the follow-up study in this experiment focused on the regulatory role of *HLCS* in adipocyte development.

Cellular-level experiments were conducted to further investigate the impact of the *HLCS* gene on adipocytes. It was found that the proliferation abilities of 3T3-L1 cells decreased following *HLCS* interference, as indicated by a decrease in CDK2 expression and an increase in P21 expression. CDK2 is crucial for cell cycle progression from the G1 to the synthesis (S) phase, while P21 inhibits cell proliferation and division, mediates G1 phase arrest, and acts as a negative regulator [29, 30]. This suggests that interference with *HLCS* may lead to proliferation arrest in the G1 phase, resulting in reduced cell proliferation. These results indicate that *HLCS* is essential for the proliferation of 3T3-L1 adipocytes.

The core of lipid droplets is primarily composed of a neutral lipid core, which is surrounded by a monolayer of phospholipids embedded with specific proteins[31]. These proteins play crucial roles in the formation, stabilization, and metabolic regulation of lipid droplets[32]. This study found that HLCS expression peaks on the second day of adipogenic differentiation, a period that coincides with the early development of lipid droplets and the formation of the neutral lipid core. Therefore, HLCS plays a significant role in lipid formation. This study also showed that adipogenic differentiation abilities decreased following *HLCS* interference in 3T3-L1 cells, as evidenced by reduced expression of FAS, PPARγ, CEBPα, and AP2. FAS is responsible for de novo regulation of fatty acid biosynthesis [33]. *PPARγ* has been identified as a pivotal gene involved in the regulation of free fatty acid uptake, trafficking, β-oxidation, and glycolysis in adipocytes [34]. CEBPα is essential for adipocyte expansion and de novo fatty acid synthesis, coordinating with PPARγ as a core regulator [35]. Therefore, these results suggest that HLCS interference inhibits de novo fatty acid synthesis, leading to reduced adipogenic differentiation.

HLCS catalyzes the covalent binding of biotin to carboxylases, and biotin is involved in the metabolism of major nutrients in the body [36]. Some clinical studies have found that HLCS deficiency is caused by mutations in the *HLCS* gene, and biotin is commonly used to treat this deficiency [14, 15]. Biotin therapy can alleviate symptoms such as metabolic acidosis, hyperammonemia, and developmental delay associated with HLCS deficiency [37] However, the molecular mechanism of biotin treatment for HLCS deficiency, particularly in adipocytes, has not been studied. Therefore, this study investigated the effect of exogenous biotin on adipogenic differentiation of 3T3-L1 cells with *HLCS* interference. We found that exogenous biotin increased HLCS expression and that biotin supplementation following *HLCS* interference could restore HLCS expression. Previous studies in rats and human cell cultures suggest that HLCS expression depends on an adequate biotin supply [38]. HLCS can catalyze the covalent binding of ACC1 and PC to biotin; ACC1 and PC are downstream carboxylases of HLCS. As a carboxylase synthetase, HLCS functions as a catalytic enzyme, and changes in its quantity could affect the catalytic process. However, whether it influences mRNA and protein expression of downstream enzymes is rarely reported. Therefore, this study focused on the effects of *HLCS* on downstream enzyme mRNA and protein levels. We found that *HLCS* regulates the expression of *ACC1* and *PC* genes. In cells with *HLCS* interference, ACC1 and PC expression levels were significantly reduced. The downregulation of ACC1 and PC indicates impaired de novo fat synthesis [39]. ACC1 converts acetyl-CoA to malonyl-CoA, which then enters the fatty acid synthesis pathway [40]. ACC1 is known to play a crucial role in intramuscular fat and triglyceride synthesis, important for energy storage and transport [41]. PC, another critical enzyme, replenishes tricarboxylic acid (TCA)

cycle intermediates, positioning the TCA cycle as a central hub in energy metabolism [39, 42]. Therefore, interference with *HLCS* inhibits de novo fatty acid synthesis and energy metabolism in 3T3-L1 cells, reducing adipogenic differentiation.

Research has found that biotin supplementation can enhance the reaction between HLCS and carboxylase, but excessive biotin intake can be harmful to the body[43, 44]. In this experiment, after the addition of 1 μL of biotin, the increase in HLCS expression may be attributed to the fact that the reaction between biotin and carboxylase requires catalysis by HLCS and the rise in biotin levels could have induced a positive feedback mechanism, leading to the upregulation of HLCS expression. Conversely, the reduction in HLCS expression under high biotin concentrations may be attributed to the fact that excessively high biotin levels can interfere with the endogenous production of the enzyme. In our study, we found that exogenous biotin promoted adipogenic differentiation in 3T3-L1 cells and increased ACC1 expression. Previous studies support these findings, showing that biotin enhances ACC1 activity, supplying more carbon donors for fatty acid synthesis and promoting this process [45]. Additionally, in *HLCS*-interfered cells, exogenous biotin mitigated the inhibition of adipogenic differentiation, notably restoring ACC1 and PC expression levels. Thus, it appears that biotin reduces the impact of *HLCS* interference on adipocytes by participating in de novo fatty acid synthesis and energy metabolism.

The glycolysis pathway is another key process in energy metabolism [46]. *PKM* and *GSK3β* are critical glycolytic genes, with GSK3β regulating glucose homeostasis and PKM serving as a major regulatory point in glycolysis [47]. Reduced expression of GSK3β and PKM leads to glycolytic disruption and decreased energy production [48]. This study showed that *HLCS* interference lowered PKM and GSK3β expression, while exogenous biotin enhanced their expression and mitigated the effects of *HLCS* interference. These results suggest that *HLCS* interference inhibits glycolysis, and that exogenous biotin alleviates this inhibition in adipocytes.

Additionally, we found that *HLCS* interference affects lipolysis in 3T3-L1 cells, which was alleviated by exogenous biotin. The balance between lipogenesis and lipolysis regulates fat accumulation and is tied to lipid metabolism dysfunction [49]. Biotin has been shown to alleviate lipid metabolism disorders [50]. Our study concludes that *HLCS* interference disrupts the lipid balance in adipocytes, resulting in lipid metabolism disorders, and that biotin supplementation helps restore this balance by accelerating lipolysis.

The MAPK pathway, which includes ERK1/2, JNK, and p38, regulates numerous cellular activities such as proliferation and adipogenic differentiation [51]. The JNK signaling pathway is associated with oxidative stress [51]. In this study, JNK protein expression was found to be very low, so this pathway was not further examined. Several studies have shown that inhibition of the p38 signaling pathway can prevent cell proliferation [52-54]. Consistent with our findings that *HLCS* interference reduced p-p38 protein expression during adipocyte proliferation.

Various studies have also shown that the ERK1/2 signaling pathway is significantly associated with adipogenic differentiation; decreased p-ERK levels downregulate the expression of adipogenesis-related genes, thereby inhibiting the differentiation of adipocytes [55-57]. *HLCS* interference promoted the expression of ERK1/2 and inhibited the expression of p-ERK1/2 during adipogenic differentiation. The addition of biotin alleviated the inhibitory effect of *HLCS* interference on p-ERK1/2 in adipocytes.

An interesting observation during this study was that in normal adipocytes, HLCS interference decreased p-p38 and p-ERK1/2 protein expression and inhibited adipogenic differentiation. However, with exogenous biotin, p-p38 and p-ERK1/2 expression decreased whereas adipogenic differentiation was promoted. Thus, while the expression trends of p-p38 and p-ERK1/2 were similar with exogenous biotin or *HLCS* interference, the effects on adipogenic differentiation were opposite. This phenomenon is not well-documented, and the specific regulatory mechanism requires further study.

In summary, this study showed that *HLCS* is an important candidate gene for pig BF development, and *HLCS* interference significantly affects adipocyte development. Exogenous biotin not only promotes *HLCS* gene expression but also influences cellular fat deposition by regulating carboxylase activity, glycolysis, fat degradation, and fat synthesis, potentially through the MAPK signaling pathway (Fig. 7).

Acknowledgments

This work was supported by Key R&D Project in Hainan Province (ZDYF2024XDNY271), Tianjin Science and Technology Plan Project (23ZYCGSN00230), National Swine Industry Technology System (CARS-35), Anhui Natural Science Foundation Project (2208085MC76), the Scientific Research Program of Tianjin Education Commission, China (2018KJ188), Fuyang Normal University scientific research platform open topic (FYKFKT24042).

References

1. Yi W, Jianfei Z, Chenchen X, Ning M, Ting H, Jinshan Z, et al. Progress towards pig nutrition in the last 27 years. J Sci Food Agric. 2018;100(14):5102-10. https://doi.org/10.1002/jsfa.9095.

2. Albendea P, Conchione C, Ursol LM, Moret S. A Study on Mineral Oil Hydrocarbons (MOH) Contamination in Pig Diets and Its Transfer to Back Fat and Loin Tissues. Animals. 2024;14(10). https://doi.org/10.3390/ani14101450.

3. Filippo B, Giuseppe M. Pearls before Swine: Plant-Derived Wastes to Produce Low-Cholesterol Meat from Farmed Pigs—A Bibliometric Analysis Combined to Meta-Analytic Studies. Foods. 2023;12(3):571-. https://doi.org/10.3390/foods12030571.

4. Huang R, Pang Q, Zheng L, Lin J, Li H, Wan L, et al. Cholesterol metabolism: physiological versus pathological aspects in intracerebral hemorrhage. Neural Regen Res. 2025;20(4):1015-30. https://doi.org/10.4103/nrr.Nrr-d-23-01462.

5. Ingaramo M, Beckett D. Purification and characterization of human holocarboxylase synthetase. The FASEB Journal. 2008;22(S2):675-. https://doi.org/10.1096/fasebj.22.2_supplement.675.

6. R R-M, S C, T MS, A V. Biotin regulates the genetic expression of holocarboxylase synthetase and mitochondrial carboxylases in rats. The Journal of nutrition. 2001;131(7):1909-13. https://doi.org/10.1093/jn/131.7.1909.

7. Ling S, Qiu WJ, Zhang HW, Liang LL, Lu DY, Chen T, et al. Clinical, biochemical, and genetic analysis of 28 Chinese patients with holocarboxylase synthetase deficiency. Orphanet J Rare Dis. 2023;18(1):48. https://doi.org/10.1186/S13023-023-02656-Y.

8. Hidenori I, Ikuko N, JunYa K, Noriko Y. Stabilization of fatty acid synthesis enzyme acetyl-CoA carboxylase 1 suppresses acute myeloid leukemia development. The Journal of clinical investigation. 2021;131(12):1-14. https://doi.org/10.1172/JCI141529.

9. Elma Z, Haejin Y, B SJ, R NE, Gaëlle L, Paulina K, et al. SIRT4 is an early regulator of branched-chain amino acid catabolism that promotes adipogenesis. Cell Rep. 2021;36(2):109345-. https://doi.org/10.1016/j.celrep.2021.109345.

10. Chang L, Xiang Z, Yu P, Yang L, Yifan Z. Pyruvate carboxylase promotes thyroid cancer aggressiveness through fatty acid synthesis. BMC Cancer. 2021;21(1):722-. https://doi.org/10.1186/S12885-021-08499-9.

11. Schrick JJ, Lingrel JB. cDNA cloning, mapping and expression of the mouse Propionyl CoA Carboxylase Beta (pccb), the gene for human type II propionic acidaemia. Gene. 2001;264(1):147-52. https://doi.org/10.1016/s0378-1119(00)00586-2.

12. Siraprapa S, Witchuda S, Polyak SW, Chareeporn A, Sarawut J. Differential growth inhibition, cell cycle arrest and apoptosis of MCF-7 and MDA-MB-231 cells to holocarboxylase synthetase suppression. Biochem Biophys Res Commun. 2022;593:108-15. https://doi.org/10.1016/J.BBRC.2022.01.049.

13. Ngoc DD, Tage O, Bjerring SA, Thomas M, Just J, N KH. Genome-wide association and systems genetic analyses of residual feed intake, daily feed consumption, backfat and weight gain in pigs. BMC Genet. 2014;15(1):27. https://doi.org/10.1186/1471-2156-15-27.

14. Nelson AT, Jones PM, Cao J. Elevated C5-hydroxy acylcarnitine in an infant girl as a result of holocarboxylase synthetase deficiency. Clinica chimica acta; international journal of clinical chemistry. 2024;560:119747-. https://doi.org/10.1016/j.cca.2024.119747.

15. KeYao L, JianPing T, YanLing J, ShuZhen Y, Bin Z, Rong W, et al. [Holocarboxylase synthetase deficiency induced by HLCS gene mutations: a rare disease study]. Zhongguo dang dai er ke za zhi = Chinese journal of contemporary pediatrics. 2023;25(4):401-7. https://doi.org/10.7499/j.issn.1008-8830.2211062.

16. Higuchi H, Maeda T, Kawai K, Kuwano A, Kasamatsu M, Nagahata H. Physiological changes in the concentrations of biotin in the serum and milk and in the physical properties of the claw horn in Holstein cows. Vet Res Commun. 2003;27(5):407-13. https://doi.org/10.1023/a:1024714322087.

17. Cemal O, Osman K, Mehmet T, Nurhan S, R KJ, Kazim S. Effect of supplementing chromium histidinate and picolinate complexes along with biotin on insulin sensitivity and related metabolic indices in rats fed a high-fat diet. Food science & nutrition. 2019;7(1):183-94. https://doi.org/10.1002/fsn3.851.

18. Senthilraja S, Anand RS, Dhasarathan G, Sudarshana R, Tamilselvan J. Autophagy inhibition by biotin elicits endoplasmic reticulum stress to differentially regulate adipocyte lipid and protein synthesis. Cell Stress Chaperones. 2019;24(2):343-50. https://doi.org/10.1007/s12192-018-00967-9.

19. Lei P, Yunyan L, Zuochen W, Yuxin D, Chunting Z, Xueli Z, et al. GPX2 Gene Affects Feed Efficiency of Pigs by Inhibiting Fat Deposition and Promoting Muscle Development. Animals. 2022;12(24). https://doi.org/10.3390/ani12243528.

20. Zhuang Z, Li S, Ding R, Yang M, Zheng E, Yang H, et al. Meta-analysis of genome-wide association studies for loin muscle area and loin muscle depth in two Duroc pig populations. PLoS ONE. 2019;14(6):e0218263. https://doi.org/10.1371/journal.pone.0218263.

21. Yang Q, Wu P, Wang K, Chen D, Zhou J, Ma J, et al. SNPs associated with body weight and backfat thickness in two pig breeds identified by a genome-wide association study. Genomics. 2019;111(6):1583-9. https://doi.org/10.1016/j.ygeno.2018.11.002.

22. Lee W, Han K-H, Kim HT, Choi H, Ham Y, Ban T-W. Prediction of average daily gain of swine based on machine learning. Journal of Intelligent and Fuzzy Systems. 2019;36(2):923-33. https://doi.org/10.3233/JIFS-169869.

23. Serão NV, Mauch ED, Onteru SK, Rothschild MF, Dekkers JCM. Genomewide association study for residual feed intake and component traits of feed efficiency in pigs divergently selected for residual feed intake. J Anim Sci. 2016;94:12-3. https://doi.org/10.2527/msasas2016-026.

24. Kai G, Shengzhong H, Zhouyan L, Zhaobo L, Sitong L, Myong CH, et al. Analysis of metabolome and transcriptome of longissimus thoracis and subcutaneous adipose tissues reveals the regulatory mechanism of meat quality in MSTN mutant castrated male finishing pigs. Meat science. 2023;207:109370-. https://doi.org/10.1016/j.meatsci.2023.109370.

25. Zi Z, Zhengqun L, Ning L, Shuqin M, Shiyue L, Zhonghao L, et al. Effects of fermented bamboo powder on growth performance, apparent digestibility, carcass traits, and meat quality in growing-finishing pigs. Livestock Science. 2023;277. https://doi.org/10.1016/j.livsci.2023.105358.

26. Chiang HL, Wu JY, Chen YT. Identification of functional single nucleotide polymorphisms in the branchpoint site. Hum Genomics. 2017;11(1):27. https://doi.org/10.1186/s40246-017-0122-6.

27. C CJ. SNPs occur in regions with less genomic sequence conservation. PloS one. 2011;6(6):e20660. https://doi.org/10.1371/journal.pone.0020660.

28. Beate K, Barbara K, M FB, Andrea H. Single nucleotide polymorphisms in DNA repair genes and putative cancer risk. Arch Toxicol. 2016;90(10):2369-88. https://doi.org/10.1007/s00204-016-1771-2.

29. Sun Y, Wang C, Wen L, Ling Z, Xia J, Cheng B, et al. Quercetin ameliorates senescence and promotes osteogenesis of BMSCs by suppressing the repetitive element-triggered RNA sensing pathway. Int J Mol Med. 2025;55(1). https://doi.org/10.3892/ijmm.2024.5445.

30. Zhang W, Liu Y, Jang H, Nussinov R. CDK2 and CDK4: Cell Cycle Functions Evolve Distinct, Catalysis-Competent Conformations, Offering Drug Targets. JACS Au. 2024;4(5):1911-27. https://doi.org/10.1021/jacsau.4c00138.

31. Benedikt K, Stephanie K, Natalia K, Christoph H, Gabriel C, Anna T, et al. Lipid droplet-mitochondria coupling via Perilipin 5 augments respiratory capacity but is dispensable for FA oxidation. J Lipid Res. 2022;63(3):100172-. https://doi.org/10.1016/J.JLR.2022.100172.

32. A OJ, Pedro C. Dynamics and functions of lipid droplets. Nature reviews Molecular cell biology. 2019;20(3):137-55. https://doi.org/10.1038/s41580-018-0085-z.

33. Nanashima N, Norikura T, Nakano M, Hata C, Horie K. Silencing of ERRα gene represses cell proliferation and induces apoptosis in human skin fibroblasts. Mol Med Rep. 2025;31(1). https://doi.org/10.3892/mmr.2024.13370.

34. Ding Y, Jie K, Xin L, Shao B. Astragaloside IV plays a neuroprotective role by promoting PPARγ in cerebral ischemia-reperfusion rats. Behav Brain Res. 2025;476:115267. https://doi.org/10.1016/j.bbr.2024.115267.

35. Jiang S, Zhang G, Miao J, Wu D, Li X, Li J, et al. Transcriptome and Metabolome Analyses Provide Insight into the Glucose-Induced Adipogenesis in Porcine Adipocytes. Curr Issues Mol Biol. 2024;46(3):2027-42. https://doi.org/10.3390/cimb46030131.

36. Mélissa D, Hélène L, Girard CL. Biotin, folic acid, and vitamin B12 supplementation given in early lactation to Holstein dairy cows: Their effects on whole-body propionate, glucose, and protein metabolism. Anim Feed Sci Technol. 2022;292:115441. https://doi.org/10.1016/J.ANIFEEDSCI.2022.115441.

37. Kim SW, Lee HJ, Choi N, Kim EK, Ko JM. Dramatic Clinical Improvement With Biotin Mega-Dose Therapy in a Neonate With Holocarboxylase Synthetase Deficiency. Molecular genetics & genomic medicine. 2024;12(8):e70002. https://doi.org/10.1002/mgg3.70002.

38. Xia M, Malkaram SA, Zempleni J. Three promoters regulate the transcriptional activity of the human holocarboxylase synthetase gene. The Journal of Nutritional Biochemistry. 2013;24(11):1963-9. https://doi.org/10.1016/j.jnutbio.2013.06.007.

39. Jarunya N, Siraprapa S, Saowaluk S, Kulthida V, Sarawut J. CRISPR Cas9-mediated ablation of pyruvate carboxylase gene in colon cancer cell line HT-29 inhibits growth and migration, induces apoptosis and increases sensitivity to 5-fluorouracil and glutaminase inhibitor. Frontiers in Oncology. 2022;12. https://doi.org/10.3389/fonc.2022.966089

40. Yang X, Huang H, Wang Z, Haslam TM, Kunst L, Wang P, et al. Acetyl-CoA Carboxylase1 Influences ECERIFERUM2 Activity to Mediate the Synthesis of Very-Long-Chain Fatty Acid Past C28. Plant Physiol. 2024. https://doi.org/10.1093/plphys/kiae253.

41. Arturo GMDI, Ernesto M, Edrei SJ, Luis BJ, Daniel H, Daniel T, et al. Effect of Zilpaterol Hydrochloride and Zinc Methionine on Growth, Carcass Traits, Meat Quality, Fatty Acid Profile and Gene Expression in Longissimus dorsi Muscle of Sheep in Intensive Fattening. Agriculture. 2023;13(3):684. https://doi.org/10.3390/AGRICULTURE13030684.

42. Zhang Y, Higgins CB, Tica S, Adams JA, Sun J, Kelly SC, et al. Hierarchical tricarboxylic acid cycle regulation by hepatocyte arginase 2 links the urea cycle to oxidative metabolism. Cell metabolism. 2024;36(9):2069-85.e8. https://doi.org/10.1016/j.cmet.2024.07.007.

43. Eugeni B, Lise V, Valentina T, Gwen F, Solia A, E AK, et al. Impairment of gut microbial biotin metabolism and host biotin status in severe obesity: effect of biotin and prebiotic supplementation on improved metabolism. Gut. 2022;71(12). https://doi.org/10.1136/GUTJNL-2021-325753.

44. Báez-Saldaña A, Camacho-Arroyo I, Espinosa-Aguirre JJ, Neri-Gómez T, Rojas-Ochoa A, Guerra-Araiza C, et al. Biotin deficiency and biotin excess: Effects on the female reproductive system. Steroids. 2009;74(10-11):863-9. https://doi.org/10.1016/j.steroids.2009.06.004.

45. Tengfei Z, Xin G, Lu M, Shengyong M, Dengpan B. Biotin and Leucine Alone or in Combination Promoted the Synthesis of Odd- and Branched-Chain Fatty Acids in the Rumen In Vitro. Agriculture. 2023;13(1). https://doi.org/10.3390/AGRICULTURE13010145.

46. Ding X, Chen C, Zhao H, Dai B, Ye L, Song T, et al. Inhibiting SHP2 reduces glycolysis, promotes microglial M1 polarization, and alleviates secondary inflammation following spinal cord injury in a mouse model. Neural Regen Res. 2025;20(3):858-72. https://doi.org/10.4103/nrr.Nrr-d-23-01925.

47. Xiao H, Fei Y, Zhengyi Z, Zhanwu H, Qiong S, Tian S, et al. 4EBP2-regulated protein translation has a critical role in high-fat diet–induced insulin resistance in hepatocytes. J Biol Chem. 2023;299(11):105315-. https://doi.org/10.1016/j.jbc.2023.105315.

48. Nedden SZ, Safari MS, Weber D, Kuenkel L, Garmsiri C, Lang L, et al. Protein kinase N1 deficiency results in upregulation of cerebral energy metabolism and is highly protective in in vivo and in vitro stroke models. Metabolism: clinical and experimental. 2024:156039. https://doi.org/10.1016/j.metabol.2024.156039.

49. Jeong KJ, Mukae M, Lee SR, Kim SY, Kim SH, Cho YE, et al. Progesterone increases hepatic lipid content and plasma lipid levels through PR- B-mediated lipogenesis. Biomedicine & pharmacotherapy = Biomedecine & pharmacotherapie. 2024;172:116281-. https://doi.org/10.1016/j.biopha.2024.116281.

50. Lise V, Jean D, Eugeni B, Camille G, Metacardis Ct, Tiphaine LR, et al. Severe Obesity Is Associated with Altered Gut Microbiota Biotin Metabolism and Host Biotin Status. The FASEB Journal. 2021;35(S1). https://doi.org/10.1096/FASEBJ.2021.35.S1.02007.

51. Liu L, Wen T, Xiao Y, Chen H, Yang S, Shen X. Sea buckthorn extract mitigates chronic obstructive pulmonary disease by suppression of ferroptosis via scavenging ROS and blocking p53/MAPK pathways. J Ethnopharmacol. 2025;336:118726. https://doi.org/10.1016/j.jep.2024.118726.

52. Zheng T, Deng J, Wen J, Xiao S, Huang H, Shang J, et al. p38α deficiency ameliorates psoriasis development by downregulating STAT3-mediated keratinocyte proliferation and cytokine production. Communications biology. 2024;7(1):999. https://doi.org/10.1038/s42003-024-06700-w.

53. Zhang T, Luo XY, Jing L, Mo C, Guo H, Yang S, et al. Toosendanin inhibits T-cell proliferation through the P38 MAPK signalling pathway. Eur J Pharmacol. 2024;973:176562-. https://doi.org/10.1016/j.ejphar.2024.176562.

54. Kumar A, Asiedu E, Hefni E, Armstrong C, Menon D, Ma T, et al. Angiopoietin-like 4 is upregulated by amphiregulin and activates cell proliferation and migration through p38 kinase in head and neck squamous cell carcinoma. Journal of oral pathology & medicine : official publication of the International Association of

Oral Pathologists and the American Academy of Oral Pathology. 2024;53(6):366-75. https://doi.org/10.1111/jop.13545.

55. Kim SY, Park SY, Kim JE. GULP1 deficiency reduces adipogenesis and glucose uptake via downregulation of PPAR signaling and disturbing of insulin/ERK signaling in 3T3-L1 cells. Journal of cellular physiology. 2024. https://doi.org/10.1002/jcp.31173.

56. Ru Z, XingHua W, BoWen W, Xuan O, YaYan Y, HuaTao X, et al. Prostaglandin F2α Regulates Adipogenesis by Modulating Extracellular Signal-Regulated Kinase Signaling in Graves' Ophthalmopathy. Int J Mol Sci. 2023;24(8). https://doi.org/10.3390/ijms24087012.

57. Mingyue S, Shuai Y, Xiaoyu H, Shouyuan W, Wenxia L, Jiale Y, et al. Caveolae-associated protein 3 promotes adipogenic differentiation of porcine preadipocytes by promoting extracellular signal-regulated kinase phosphorylation. Animal science journal = Nihon chikusan Gakkaiho. 2023;94(1):e13822-e. https://doi.org/10.1111/asj.13822.

546 **Table 1.** Genetic diversity and genotype frequency of 5 SNPs of *HLCS* in 592 Duroc pigs

SNPs	Numbers	Genotype frequency			χ^2	*PIC*	*He*	*Ne*
ASGA0089950	592	CC	CT	TT	1.63	0.24	0.28	1.38
		0.69	0.29	0.02				
ASGA0097399	592	CC	GC	GG	1.63	0.24	0.28	1.38
		0.69	0.29	0.02				
ALGA0073814	592	GG	GT	TT	6.16	0.32	0.39	1.65
		0.51	0.44	0.05				
ASGA0059961	591	AA	AG	GG	5.59	0.32	0.40	1.66
		0.51	0.43	0.05				
ALGA0073818	591	TT	TG	GG	5.59	0.32	0.40	1.66
		0.51	0.43	0.05				

547 $\chi_{0.05}^2 = 5.991$, $\chi_{0.01}^2 = 9.21$. *PIC*: polymorphism information content, *He*: gene heterozygosity, *Ne*: effective number
548 of alleles.
549

550

551 **Table 2.** Association of genotype of *HLCS* 5 SNPs with 100 kg BF in 592 Duroc pigs

SNPs	Genotype	Num.	Phenotypic value [1)]	Genotype	Num.	EBV [1)]
ASGA0089950	CC	384	7.86 ± 0.08[b]	CC	384	-0.00 ± 0.00[b]
	CT	182	7.68 ± 0.10[b]	CT	182	-0.01 ± 0.00[b]
	TT	26	8.60 ± 0.38[a]	TT	26	0.02 ± 0.01[a]
ASGA0097399	CC	384	7.86 ± 0.08[b]	CC	384	-0.00 ± 0.00[b]
	CG	182	7.68 ± 0.10[b]	GC	182	-0.01 ± 0.00[b]
	GG	26	8.60 ± 0.38[a]	GG	26	0.02 ± 0.01[a]
ALGA0073814	GG	346	7.74 ± 0.08	GG	346	-0.01 ± 0.00
	GT	221	7.95 ± 0.11	GT	221	-0.00 ± 0.00
	TT	25	8.29 ± 0.27	TT	25	0.01 ± 0.01
ASGA0059961	AA	345	7.73 ± 0.08	AA	345	-0.01 ± 0.00
	AG	221	7.95 ± 0.11	AG	221	-0.00 ± 0.00
	GG	25	8.29 ± 0.27	GG	25	0.01 ± 0.01
ALGA0073818	TT	345	7.73 ± 0.08	TT	345	-0.01 ± 0.00
	TG	221	7.95 ± 0.11	TG	221	-0.00 ± 0.00
	GG	25	8.29 ± 0.27	GG	25	0.01 ± 0.01

552 [1)]The value of each trait is expressed as mean ± standard error. [a,b]$P < 0.05$.

553

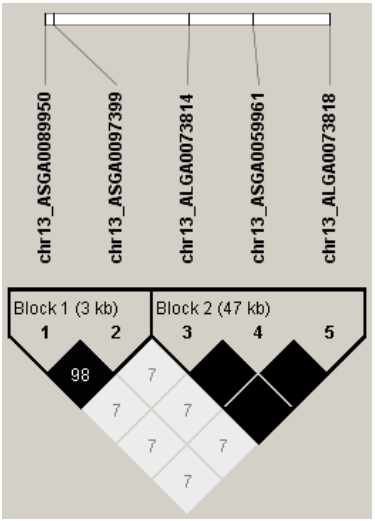

Fig. 1. Linkage disequilibrium and haplotype block analysis using the 5 SNPs for *HLCS* in 592 Duroc pigs. Solid lines indicate the block identified. The diamonds represent linkage disequilibrium between each SNP.

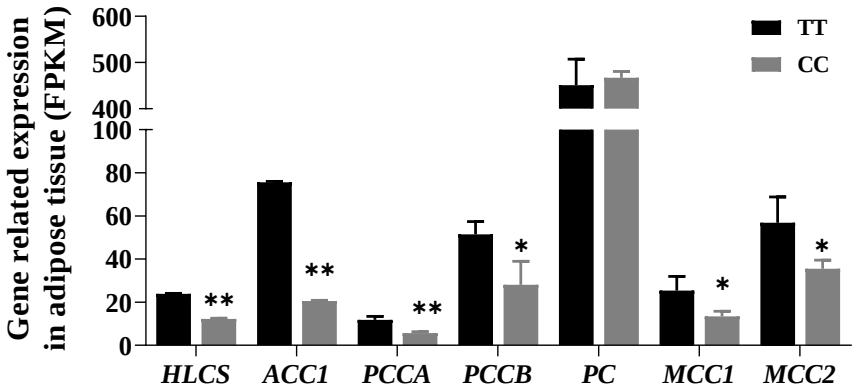

Fig. 2. mRNA expression of *HLCS* (ASGA0089950) in adipose tissue for genotypes CC and TT in Duroc pigs. **P* < 0.05, ***P* < 0.01.

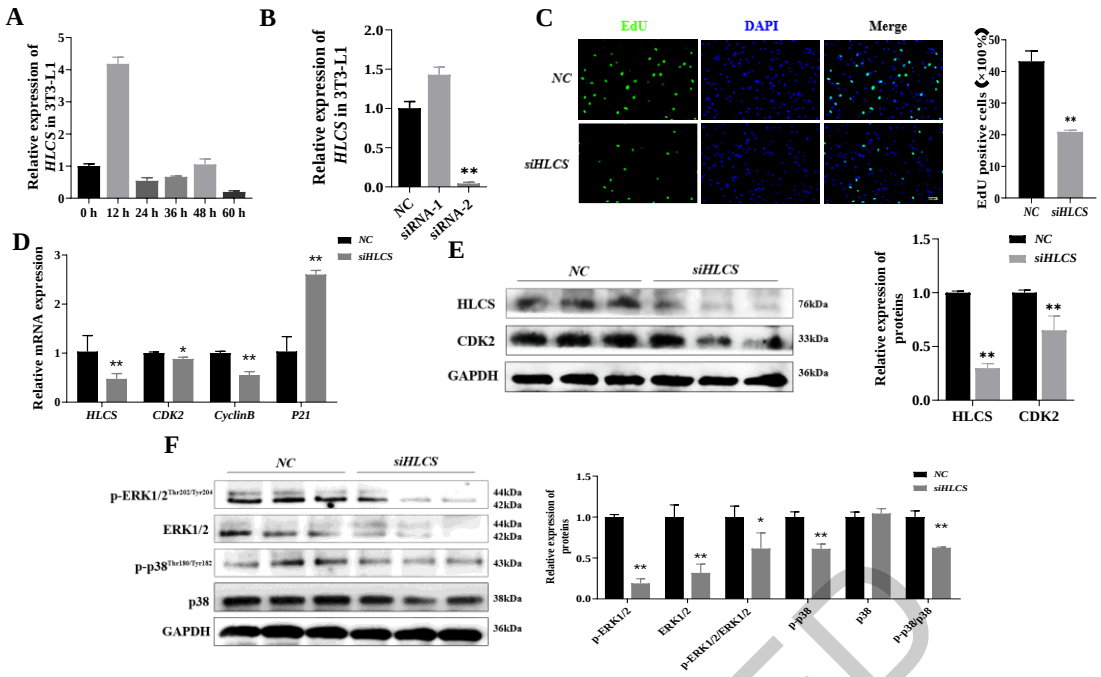

Fig. 3. *HLCS* interference inhibited the proliferation of 3T3-L1 cells. (A) The expression profile of *HLCS* during the proliferation phase of 3T3-L1 cells. mRNA expression of *HLCS* was measured at 0, 12, 24, 36, 48, and 60 h of proliferation in 3T3-L1 cells. (B) *HLCS* expression in 3T3-L1 cells at 24 h after *siHLCS* transfection. (C) Representative immunostaining images comparing proliferating cells in the NC group and *HLCS* interference group; nuclei were stained with Hoechst 33342. Green represents EdU staining, and blue represents nuclear staining, with quantification of the percentage of EdU-positive cells. n = 10. Scale bar, 100 μm. (D) The expression levels of *HLCS*, *CDK2*, *Cyclin B*, and *P21* were measured by qRT-PCR, with *GAPDH* as the normalization control. (E) Western blot analysis showing protein expression of HLCS and CDK2, including protein grayscale analysis. (F) Protein expression levels of p-ERK1/2, ERK1/2, the p-ERK1/2 to ERK1/2 ratio, p-p38, p38, and the p-p38 to p38 ratio in proliferating 3T3-L1 cells. GAPDH served as an internal control. Data are expressed as mean ± SD. n = 3, **P* < 0.05, ***P* < 0.01.

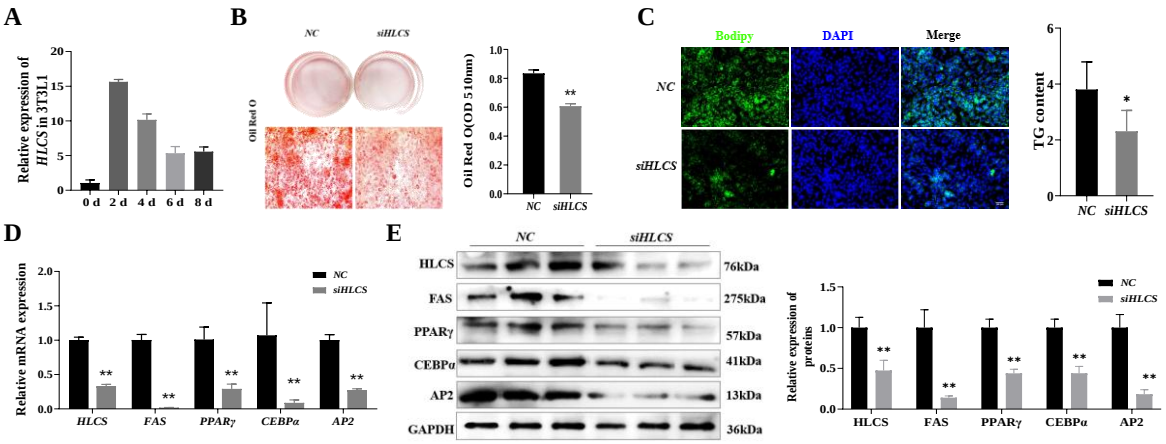

Fig. 4. *HLCS* interference inhibited adipogenic differentiation of 3T3-L1 cells. 3T3-L1 cells were transfected with *siHLCS* and induced to differentiate following cell contact inhibition. (A) Expression profile of *HLCS* during the differentiation stages of 3T3-L1 cells. mRNA expression levels were measured at 0, 2, 4, 6, and 8 days of differentiation. (B) After 6 days of adipogenic differentiation induction, Oil Red O staining was used to evaluate lipid droplet production, with absorbance measured at 510 nm. (C) Representative image of Bodipy staining. Lipid droplets are stained with Bodipy (green), and nuclei are stained with DAPI (blue), n = 10. Scale bar, 100 μm. (D) qRT-PCR analysis of *FAS*, *PPARγ*, *CEBPα*, and *AP2* gene expression, with *GAPDH* as the normalization control. (E) Western blot analysis of FAS, PPARγ, CEBPα, and AP2 protein expression, with protein grayscale analysis. GAPDH served as an internal control. Data are expressed as mean ± SD. n = 3, $*P < 0.05$, $**P < 0.01$.

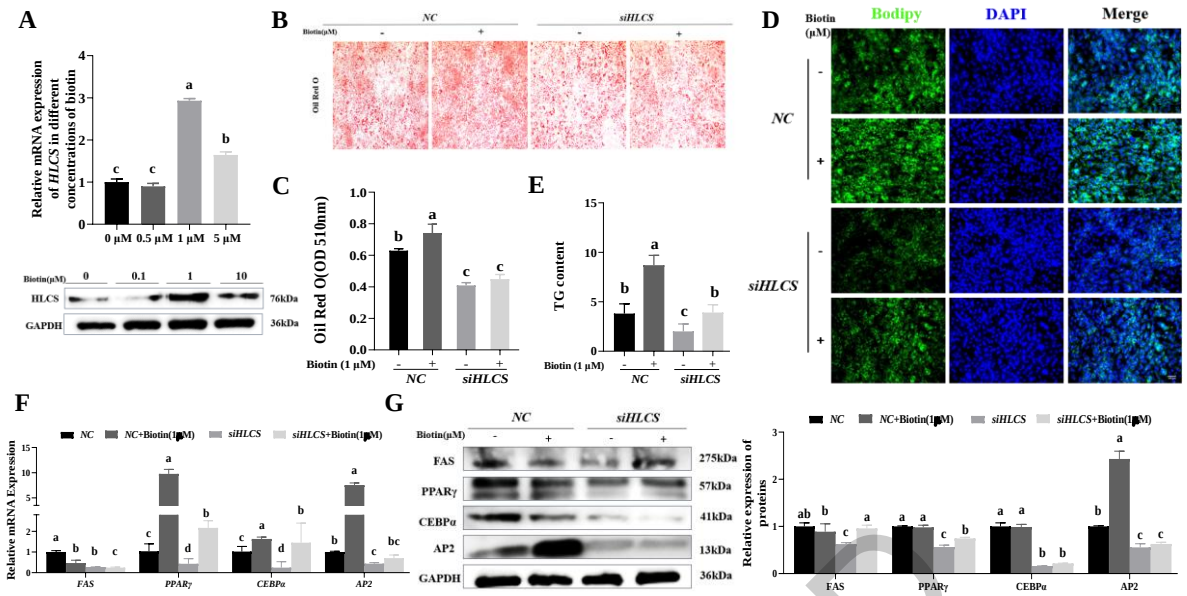

Fig. 5. Exogenous biotin promoted *HLCS* expression and alleviated the inhibition of adipogenic differentiation caused by *HLCS* interference in 3T3-L1 cells. (A) Western blot analysis of HLCS protein expression after the addition of different biotin concentrations. (B) After 6 days of adipogenic differentiation induction, Oil Red O staining was used to evaluate lipid droplet production. (C) Oil Red O absorbance at 510 nm. (D) Representative Bodipy-stained image showing lipid droplets stained with Bodipy (green) and nuclei stained with DAPI (blue), n = 10. Scale bar, 100 μm. (E) Quantification of Bodipy fluorescence intensity. (F) qRT-PCR analysis of *FAS*, *PPARγ*, *CEBPα*, and *AP2* gene expression. (G) Western blot analysis of FAS, PPARγ, CEBPα, and AP2 protein expression, with grayscale analysis of HLCS, FAS, PPARγ, CEBPα, and AP2 proteins. Different letters indicate significant differences ($P < 0.05$). Data are presented as mean ± SD (n = 3).

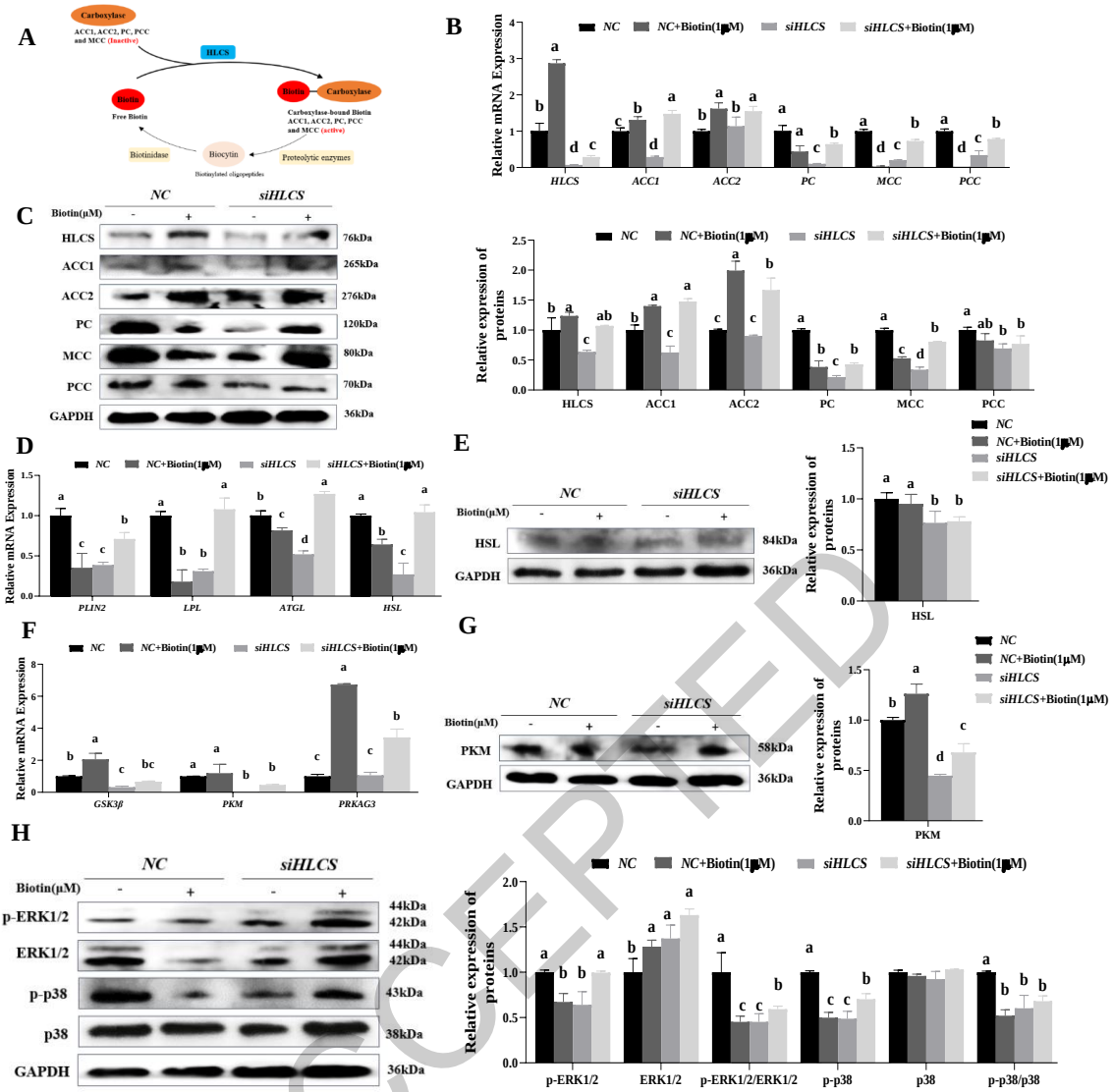

Fig. 6. Effect of biotin combined with HLCS on carboxylase, lipolysis, glycolysis, and MAPK signaling pathways after adipogenic differentiation of 3T3-L1 cells. (A) Schematic diagram of the biotin cycle, showing HLCS catalyzing the covalent binding of biotin to carboxylases, leading to their biotinylation. (B) mRNA expression of *ACC1*, *ACC2*, *PC*, *PCC*, and *MCC* as detected by qRT-PCR. (C) Protein expression of ACC1, ACC2, PC, PCC, and MCC, with grayscale analysis of these proteins detected by western blotting. (D) mRNA expression of *PLIN2*, *LPL*, *ATGL*, and *HSL* as detected by qRT-PCR. (E) Protein expression of *HSL*, including grayscale analysis, as detected by western blotting. (F) mRNA expression of *GSK3β*, *PKM*, and *PRKAG3* genes detected by qRT-PCR. (G) Protein expression of PKM and grayscale analysis of PKM detected by western blotting. (H) Protein expression of p-ERK1/2, ERK1/2, p-p38, and p38, including grayscale analysis of p-ERK1/2, ERK1/2, and p-p38/p38 ratios. Different letters indicate significant differences ($P < 0.05$). Data are presented as mean ± SD (n = 3).

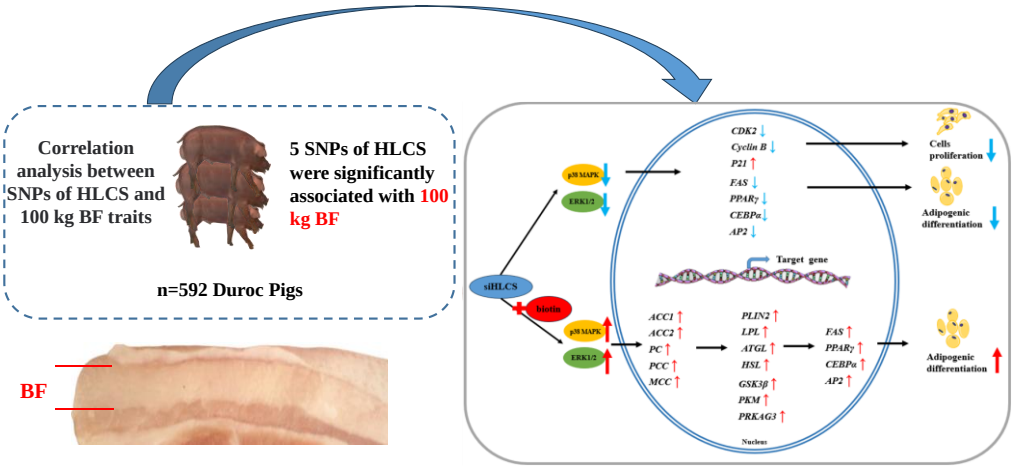

Fig. 7. Hypothetical model illustrating the role of *HLCS* in regulating 100-kg BF in pigs through adipocyte development. The left dotted box shows that five SNPs of *HLCS* are significantly associated with 100-kg BF in Duroc pigs. Interfering with *HLCS* inhibits adipocyte proliferation and fat deposition. Exogenous biotin influences cellular fat deposition by regulating carboxylase activity, glycolysis, fat degradation, and fat synthesis, potentially via the MAPK signaling pathway (mechanism diagram on the right). ↑ Indicates upregulated expression; ↓ Indicates downregulated expression.